Heliyon 10 (2024) e36831

Contents lists available at ScienceDirect

Heliyon

journal homepage: www.cell.com/heliyon

Research article

Construction of a NETosis-related gene signature for predicting the prognostic status of sepsis patients

Jiahao Wu [1], Xingxing Cao [1], Linghui Huang [*], Yifeng Quan [**]

Department of Rehabilitation, Northern Jiangsu People's Hospital Affiliated to Yangzhou University, 225002, China

ARTICLE INFO

Keywords:
Sepsis
NETosis
Prognosis
Riskscore
Pathway
Immunoinfiltration

ABSTRACT

Background: Sepsis is a common traumatic complication of response disorder of the body to infection. Some studies have found that NETosis may be associated with the progression of sepsis.
Methods: Data of the sepsis samples were acquired from Gene Expression Omnibus (GEO) database. Gene set enrichment score was calculated using single-sample gene set enrichment analysis (ssGSEA). Weighted gene co-expression network analysis (WGCNA), protein-protein interaction (PPI) networks analysis, and stepwise multivariable regression analysis were performed to identify NETosis-associated genes for sepsis prognosis. To assess the infiltration of immune cells, the ESTIMATE and CIBERPSORT algorithms were used. Functional enrichment analysis was conducted in the clusterProfiler package.
Results: Different programmed death pathways were abnormally activated in sepsis patients as compared to normal samples. We screened five important NETosis associated genes, namely, CEACAM8, PGLYRP1, MAPK14, S100A12, and LCN2. These genes were significantly positively correlated with entotic cell death and ferroptosis and negatively correlated with autophagy. A clinical prognostic model based on riskscore was established using the five genes. The ROC curves of the model at 7 days, 14 days and 21 days all had high AUC values, indicating a strong stability of the model. Patients with high riskscore had lower survival rate than those with low riskscore. After the development of a nomogram, calibration curve and decision curve evaluation also showed a strong prediction performance and reliability of the model. As for clinicopathological features, older patients and female patients had a relatively high riskscore. The riskscore was significantly positively correlated with cell cycle-related pathways and significantly negatively correlated with inflammatory pathways.
Conclusion: We screened five NETosis-associated genes that affected sepsis prognosis, and then established a riskscore model that can accurately evaluate the prognosis and survival for sepsis patients. Our research may be helpful for the diagnosis and clinical treatment of sepsis.

1. Introduction

Sepsis is a critical condition caused by dysfunctional organ response to infection, posing a significant worldwide health issue [1]. In the United States, sepsis stands as the leading cause of mortality within hospitals [2,3]. Although the actual prevalence of sepsis

* Corresponding author.
** Corresponding author.
E-mail addresses: hlhzhenjiu@163.com (L. Huang), 56201981@qq.com (Y. Quan).
[1] Equal Contribution.

https://doi.org/10.1016/j.heliyon.2024.e36831
Received 24 November 2023; Received in revised form 22 August 2024; Accepted 22 August 2024
Available online 23 August 2024

remains unclear, evidence indicates that preventative initiatives targeting both community-acquired and healthcare-associated infections play a significant role in lowering the disease's occurrence [4,5]. The clinical management of sepsis involves administering antibiotics, correcting acidosis, providing fluid resuscitation and support, utilizing hemoperfusion therapy, and implementing mechanical ventilation [6]. A challenge is currently faced in the development of innovative treatments. Despite the administration of potent antibiotics for sterilization, the ensuing cascade of inflammatory factors cannot be halted, potentially leading to the patient's demise in a short span of time [7]. While updated diagnostic guidelines for sepsis were released in 2016, the diagnostic and prognostic capabilities of conventional biomarkers like procalcitonin (PCT) and lactic acid remain uncertain [8], calling for the urgent identification of new biomarkers.

NETosis is a regulated program for the formation of neutrophils extracellular trap (NET) that helps the body to capture pathogens in external environment and achieve immunity from foreign invasion [9]. NET is a network structure containing chromatin in which neutrophils participate in the modification process after the release of a variety of different physiological function proteins in immune response and can help realize the immune defense in the body [10]. The main inducers of NETosis include the invasion of pathogens such as bacteria, immune complexes composed of antibodies, hormones, foreign bodies and other physiological stimuli [11]. The production of NETosis is closely related to the inflammatory response, bacterial and fungal infections, and autoimmune diseases as well as subsequent signaling pathway activation and immune regulation [12]. NETosis can help the body to achieve defense and immune functions, but at the same time, it might lead to tissue and organ damage in some extreme cases [13].

This study identified genes related to sepsis prognosis based on the data from Gene Expression Omnibus (GEO) database using single-sample gene set enrichment analysis (ssGSEA), weighted gene co-expression network analysis (WGCNA), and protein-protein interactions (PPI) methods. A NETosis-associated risk model was established to assess the prognosis of sepsis patients, providing new insights into the clinical management and treatment of sepsis.

2. Material and methods

2.1. Download of sepsis transcriptome data

Clinical information and transcription profiles of patients with sepsis were acquired from the Gene Expression Omnibus (GEO) (https://www.ncbi.nlm.nih.gov/) database to select samples with clinical information such as gender, age, overall survival (OS) and survival status were retained [14]. Subsequently, we downloaded four GEO datasets (GSE57065, GSE95233, GSE185263, and GSE65682) for further study. The clinical information of the samples was displayed in Table 1.

2.2. Sepsis transcriptome data processing

For GEO cohort, all raw data of the microarray dataset were downloaded from the GEO database. The R software oligo package was used for background correction, quantile normalization, and log2 transformation, and all microarray datasets were normalized by Robust Multi-array Average algorithm [15,16]. First, CEL files were read by the "read.celfiles" function with default mode parameters. Next, the function "rma" was processed with the parameters of background = "TRUE", normalize = "TRUE", subset = "NULL", target = "core". Finally, the probe was mapped to the gene according to the annotation file of the chip, and the median was taken when multiple probes were mapped to the same gene, while a probe was deleted when one probe could be mapped to multiple genes.

2.3. Enrichment analysis

The genes associated with programmed death were derived from a previous study [17], and we used R software GSVA package to conduct ssGSEA to calculate the gene set enrichment score [18]. At the same time, "hallmark gene sets" from the Molecular Signatures Database (MsigDB) database was downloaded to compute the pathway enrichment score of the sample [19]. Furthermore, the relationship between the NTEosis-related signature genes and different pathways was analyzed applying clusterProfiler package (version 3.14.3) and the results were visualized into heatmaps using "enrichplot" [20]. The parameters of the "enrichGO" function were as follows: OrgDb = "org.Hs.eg.db", keyType = "SYMBOL", minGSSize = 10, maxGSSize = 500, ont = "ALL", pvalueCutoff = 0.05, pAdjustMethod = "BH", qvalueCutoff = 0.2. The parameters of the "enrichKEGG" function are set to organism = "hsa", keyType = "kegg", minGSSize = 10, maxGSSize = 500, pvalueCutoff = 0.05, pAdjustMethod = "BH", qvalueCutoff = 0.2.

Table 1
Clinical information of 4 groups of GEO cohort.

Accession	Sample (N)	Age	Gender (percent male)	Outcome
GSE57065	107	58 (19–84)	56 %	NA
GSE95233	214	63 (25–85)	59 %	Survivor:68, Non survivor:34
GSE185263	392	59 (18–96)	56 %	Survivor:293, Non survivor:52
GSE65682	802	63 (17–93)	59 %	Survivor:365, Non survivor:114

2.4. Key gene modules of NETosis were identified by WGCNA analysis

Gene modules associated with NETosis in sepsis were sectioned by constructing a prognostic score model. The median absolute deviation (MAD) value of all protein-coding genes in the whole genome of all the samples were calculated. The MAD value is a reliable measure for the degree of diffusion of a set of data, with a larger MAD value indicating more variable data across samples [21,22]. Here, in order to include more genes, we chose genes with MAD greater than 70 % were considered as having potential abnormal expression and then subjected to WGCNA [23,24]. The appropriate soft threshold β was calculated to meet the standard of a scale-free network. In addition, the weighted adjacency matrix was transformed into topological overlap matrix (TOM), and the dynamic tree-cutting method was used to classify the modules. The correlation of each module with the NETosis score was computed to determine NETosis-correlated modules.

2.5. A NETosis-associated signature and construction of a prognostic model

Limma analysis of differentially expressed genes (DEGs) between the sepsis and healthy groups. A protein-protein interaction (PPI) network analysis was performed by taking the intersection of the DEGs and those in the modules significantly correlated with NETosis [25]. The PPI network of the generated DEGs identified from the STRING database was developed to screen key proteins with high centrality. Subsequently, functionally dense network modules were identified using Cytoscape software and the molecular complex detection (MCODE) plugin. The parameters of MCODE were set to "Degree Cutoff" = 2, "K-Core" = 2, "Max. Depth" = 100, and "Node Score Cutoff" = 0.2. The key genes in the PPI network served as candidate variables to perform multivariate stepwise regression analysis using the "step" function. The regression coefficient for each selected gene was used to develop the final riskscore model as follows:

$$RiskScore = \sum_{i=1}^{n} Coei * Expi$$

(n = 7, Coei represented the corresponding Cox regression coefficient, and Expi represented the expression level of the corresponding gene). Furthermore, ROC analysis of the riskscore for prognostic classification was conducted with the R software timeROC package [26].

2.6. Construction of a nomogram

To further investigate whether the riskscore was an independent clinical prognostic factor independent of other factors (age and sex), univariate and multivariate Cox regression analyses were performed for GSE65682. Combining the riskscore and other clinicopathological features, a nomogram was established.

2.7. Assessment of immune infiltrating cells

To further assess the relationship between the seven NETosis-related key genes and immune cell infiltration, we used the ESTIMATE and CIBERSORT algorithms combined with Pearson correlation analysis for evaluation. The ESTIMATE algorithm predicts tumor purity by analyzing gene expression data in tumor tissue and estimates the level of infiltration of mesenchymal and immune cells in the tumor microenvironment [27]. The CIBERSORT algorithm uses linear support vector regression to estimate the abundance of different immune cell types in a sample by comparing it to the expression profiles of 22 known cell types [28].

2.8. Statistic analysis

All statistical data in this study were analyzed using R software (version 3.6.0). We used Wilcoxon rank-sum and signed-rank tests to compare the variability of continuous variables between two groups, and the Kruskal-Wallis rank-sum test for use in comparing the variability of continuous variables between multiple groups. Sangerbox (http://sangerbox.com/home.html) also offered auxiliary analysis in this paper, including correlation and pathway enrichment analyses [29].

3. Results

3.1. Enrichment of programmed death pathways in sepsis

Different programmed death pathways were abnormally activated in patients with sepsis as compared to normal samples in GSE57065, GSE95233, GSE185263, and GSE65682 datasets (Fig. 1A, B, C, D). At the same time, we also found that there were significant differences in programmed death pathway enrichment scores among different sepsis subtypes, and Mars 1 subtype had the highest enrichment score of programmed death pathway in GSE65682 dataset (Fig. 1E). In addition, we also analyzed the activation status of programmed death pathways between different sepsis subtypes, and found that survivor patients in Mars 1 subtype had an overall lower enrichment score of programmed death pathways in GSE65682 dataset (Fig. 1F). The netotic cell death of survivor patients in Mars 2–4 subtype were significantly less than that of non-survivor patients in GSE65682 dataset (Fig. 1G). In GSE185263

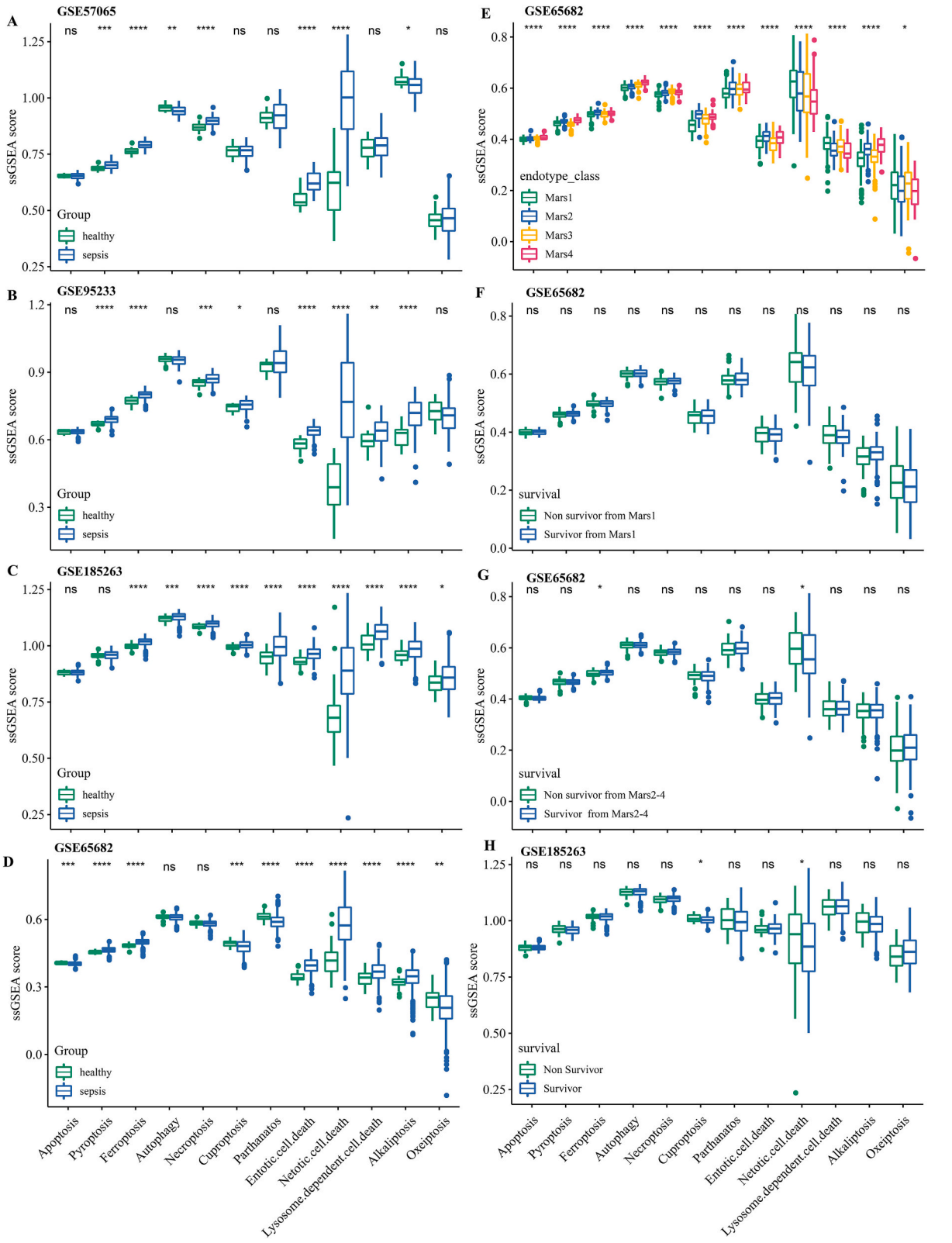

(caption on next page)

Fig. 1. Enrichment analysis of programmed death pathways in sepsis.
A–D: ssGSEA analysis on 12 programmed death pathways between healthy and sepsis in the GSE57065, GSE95233, GSE185263 and GSE65682 datasets. E: ssGSEA analysis on 12 programmed death pathways among Mars1-4 in the GSE65682 dataset. F: 12 programmed death pathway enrichment ssGSEA scores of Survivor and Non Survivor patients in Mars 1 subtype from GSE65682 dataset. G: 12 programmed death pathway enrichment ssGSEA scores of Survivor and Non Survivor patients in Mars 2–4 subtypes from GSE65682 dataset. H: 12 programmed death pathway enrichment ssGSEA scores of Survivor and Non Survivor patients in GSE185263 dataset.

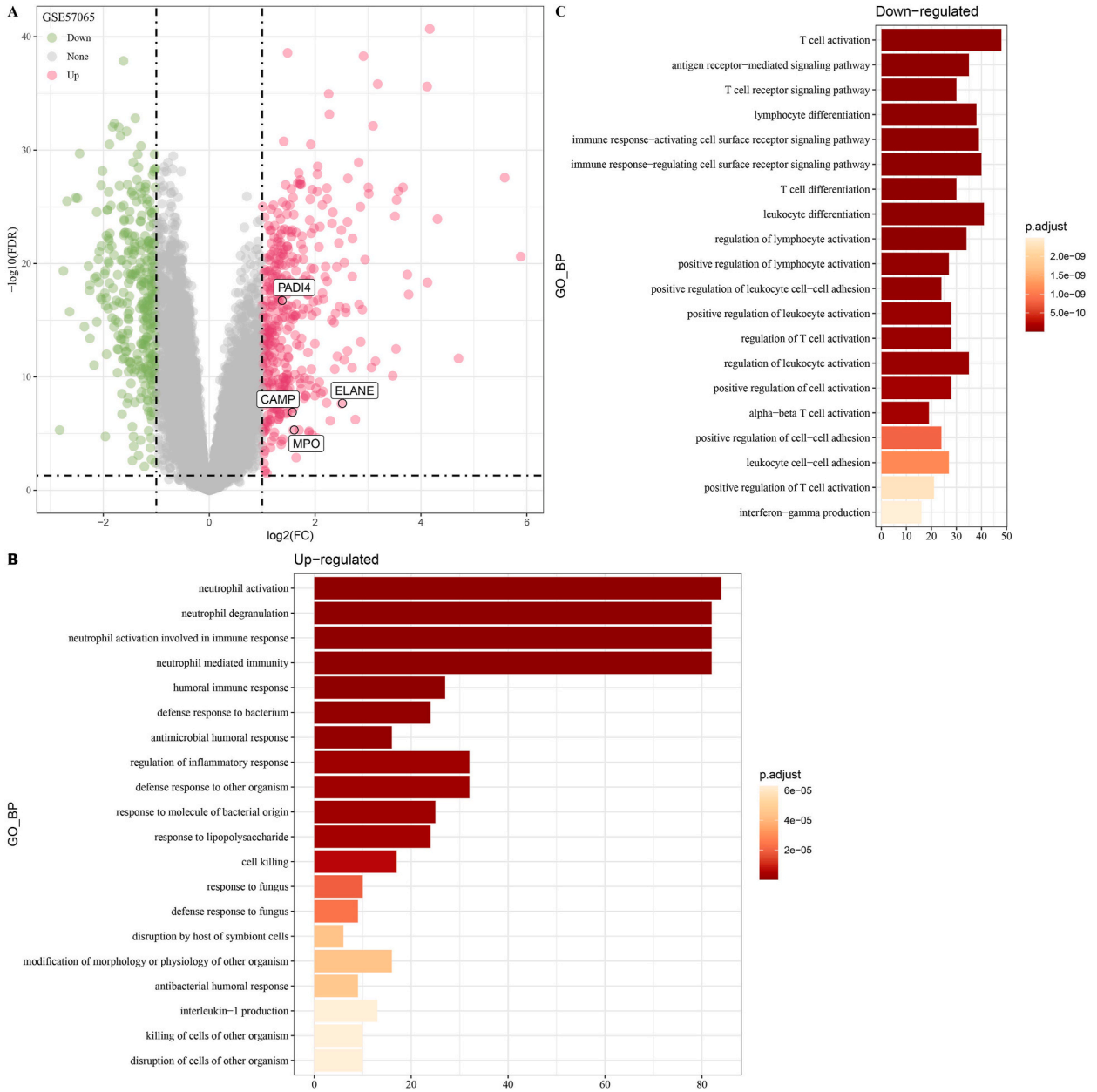

Fig. 2. Abnormal activation of neutrophil related pathways in patients with sepsis.
A: Volcano map of differentially expressed genes between patients with sepsis and normal samples in the GSE57065 cohort, in which the labeled genes are NETsis associated genes; B: Functional enrichment results of patients with Sepsis in the GSE57065 cohort; C: Functional enrichment results of sepsis patients in the GSE57065 cohort.

dataset, we further analyzed the activation status of programmed death pathway between different survival in sepsis patients, and found that compared with non-survivors, survivors had less netotic cell death and cuproptosis (Fig. 1H).

3.2. Abnormal activation of neutrophil-related pathways in patients with sepsis

Analysis of DEGs between patients with sepsis and normal controls revealed significant differences in a total of 759 genes, including 343 down-regulated genes and 416 up-regulated genes (Fig. 2A). Further functional enrichment analysis on these genes showed that up-regulated genes were significantly enriched in the pathways related to neutrophil activation, such as neutrophil degranulation, neutrophil activation involved in immune response, neutrophil activation, neutrophil mediated immunity, etc. (Fig. 2B), while down-regulated genes were significantly enriched to T cell-related biological pathways, such as alpha-beta T cell activation, T cell activation, T cell receptor signaling pathway, etc. (Fig. 2C).

3.3. Identification of NETosis-associated gene modules

To ensure a scale-free network when constructing the gene co-expression network, the soft threshold β was selected as 7 (Figs. S1A–B). Network analysis sectioned 19 gene modules. As shown in different colors, the heatmaps showed the characteristic gene adjacency of the module (Figs. S1C–D). In addition, the correlation between modules and sample types (sepsis and heathy), NETosis, age and gender were also computed. Among them, blue module showed the most significant correlation with sample types and NETosis (Fig. 3A), as its correlation coefficient between gene significance (GS) and module membership (MM) reached 0.64 (Fig. 3B). This suggested that these gene modules were built with a high quality. Here, we obtained a total of 735 module genes. Subsequently, 231 genes in the intersection of these 735 genes and 759 DEGs were taken for further analysis. Notably, 219 of the 231 genes were differentially up-regulated and 12 were differentially down-regulated in sepsis patients (Fig. 3C).

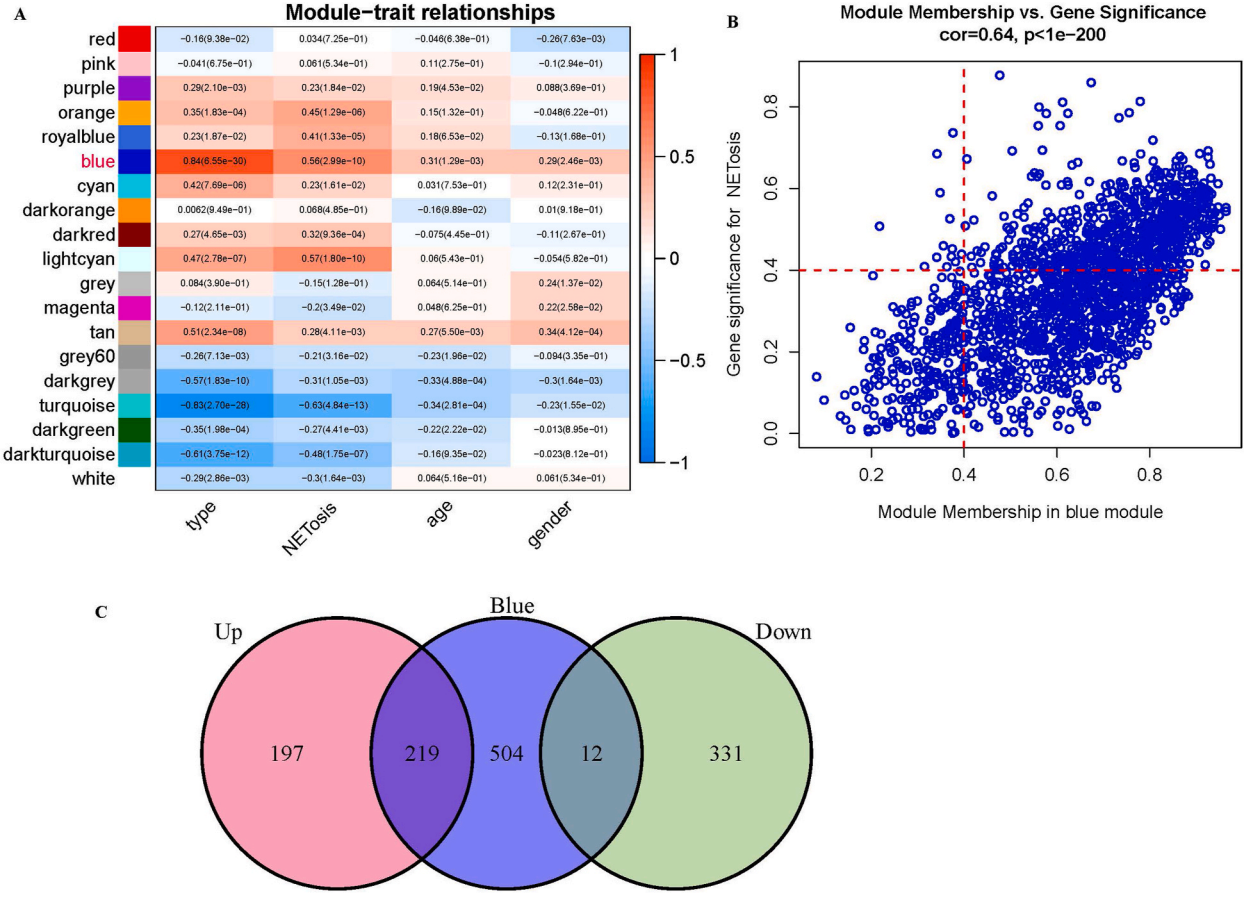

Fig. 3. Identification of NETosis associated gene modules.
A: Correlation analysis between module eigengenes and clinical traits in GSE57065; B: The high correlation between GS and MM in the blue modulein GSE57065 ($P < 0.0001$). Statistic test: Pearson correlation coefficient, two-sided unpaired *t*-test; C: Distribution of key genes and differentially expressed genes of blue model in GSE57065. (For interpretation of the references to color in this figure legend, the reader is referred to the Web version of this article.)

3.4. PPI network construction and module-based network analysis of potential targets

By intersecting the key genes of the blue module with the DEGs, we identified 231 common genes. Further, we performed PPI network analysis for these 231 genes. A total of 174 targets in STRING database were in the intersection under a confidence score >0.4. After deleting nodes with few edges in the network, further analysis selected 163 targets (Fig. 4A). Detailed topological parameters of these 163 targets were displayed. Functional enrichment analysis on these 163 genes were performed, and we found that these genes were significantly enriched to neutrophil-related biological processes (Fig. 4B–E). Densely connected protein groups in the network of potential targets were determined by mature MCODE algorithm. We extracted two functional modules using the 163 targets (Fig. 4F and G).

3.5. Identification of NETosis-associated genes

The topological features of all nodes in the above PPI network were computed by Cytoscape. Normally, nodes with the highest level of topological parameter degree, meso-centrality and near-centrality were regarded as the core targets. Therefore, in this study, we screened 10 core target genes for nodes with higher topological parameters. As shown in Table 2. Subsequently, we used the MCODE plugin to further filter clusters of nodes tightly structured and topologically important in the PPI network (Cluster1 and Cluster2). Genes from these two clusters and the 10 core target genes were used to take the intersection, and finally a total of 7 key genes were obtained. (Fig. 5A). In addition, we performed ROC analysis on these 7 key genes. It can be seen that in the GSE57065 cohort, these 7 genes can well distinguish sepsis from healthy samples. Among them, the AUC of PGLYRP1, MMP8, MAPK14 and S100A12 genes was close to 1, showing a significant classification ability (Fig. 5B). Meanwhile, we also analyzed the expression of these 7 genes in different sample types, and it can be seen that the expression of these 7 genes in sepsis is significantly higher than that in healthy samples (Fig. 5C–I).

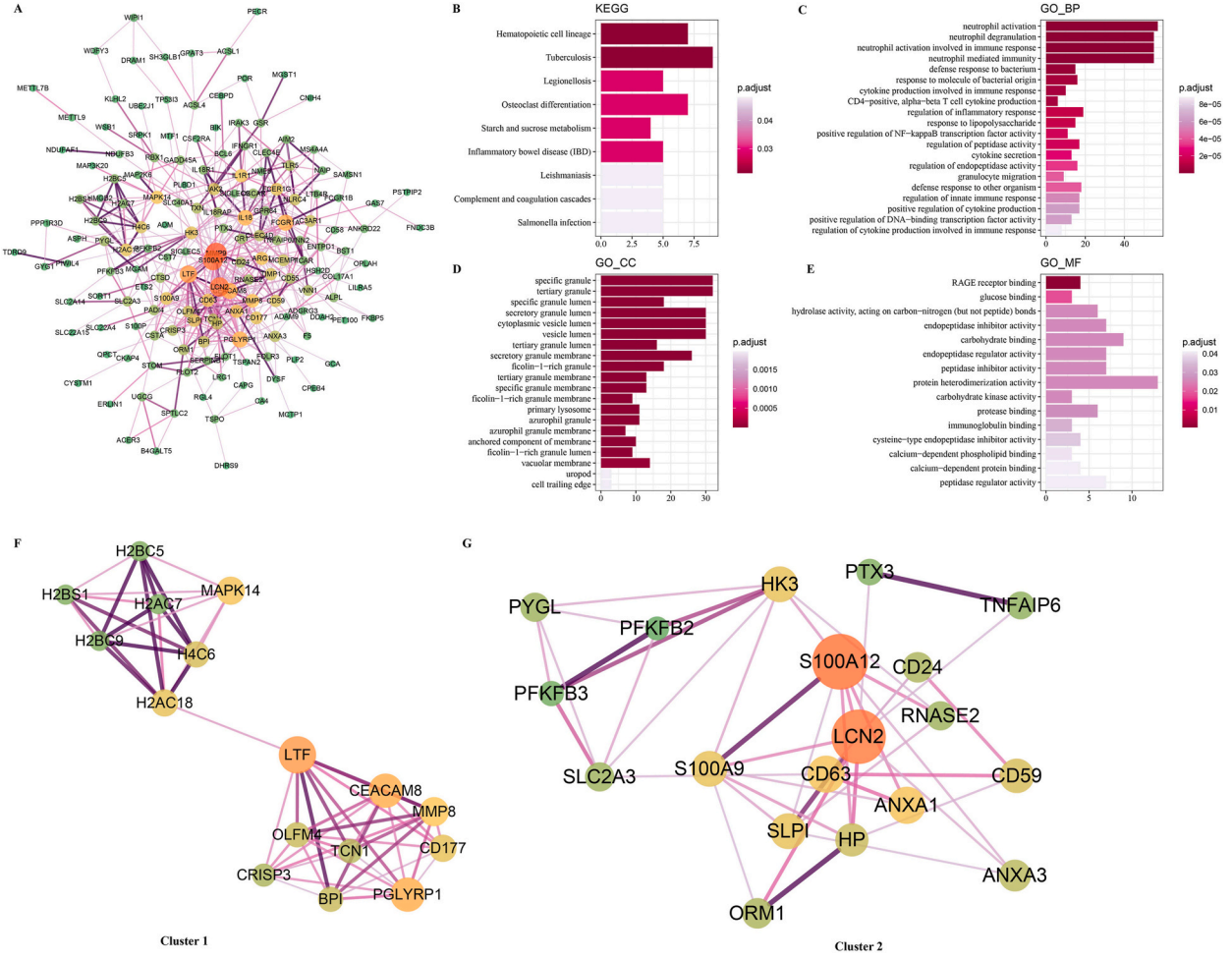

Fig. 4. PPI network construction and identification of functional modules.
A: PPI network; B–E: Functional enrichment analysis of 163 targets; F–G: Two functional modules identified by MCODE.

Table 2
Topological Parameters of core Genes in the PPI Network.

	Gene	Degree	BetweennessCentrality	ClosenessCentrality
1	MMP9	31	0.181	0.451
2	S100A12	28	0.138	0.43
3	LCN2	27	0.086	0.406
4	LTF	23	0.068	0.408
5	FCGR1A	20	0.079	0.396
6	CEACAM8	20	0.043	0.382
7	PGLYRP1	20	0.037	0.379
8	IL18	19	0.071	0.409
9	MMP8	15	0.008	0.367
10	MAPK14	14	0.084	0.364

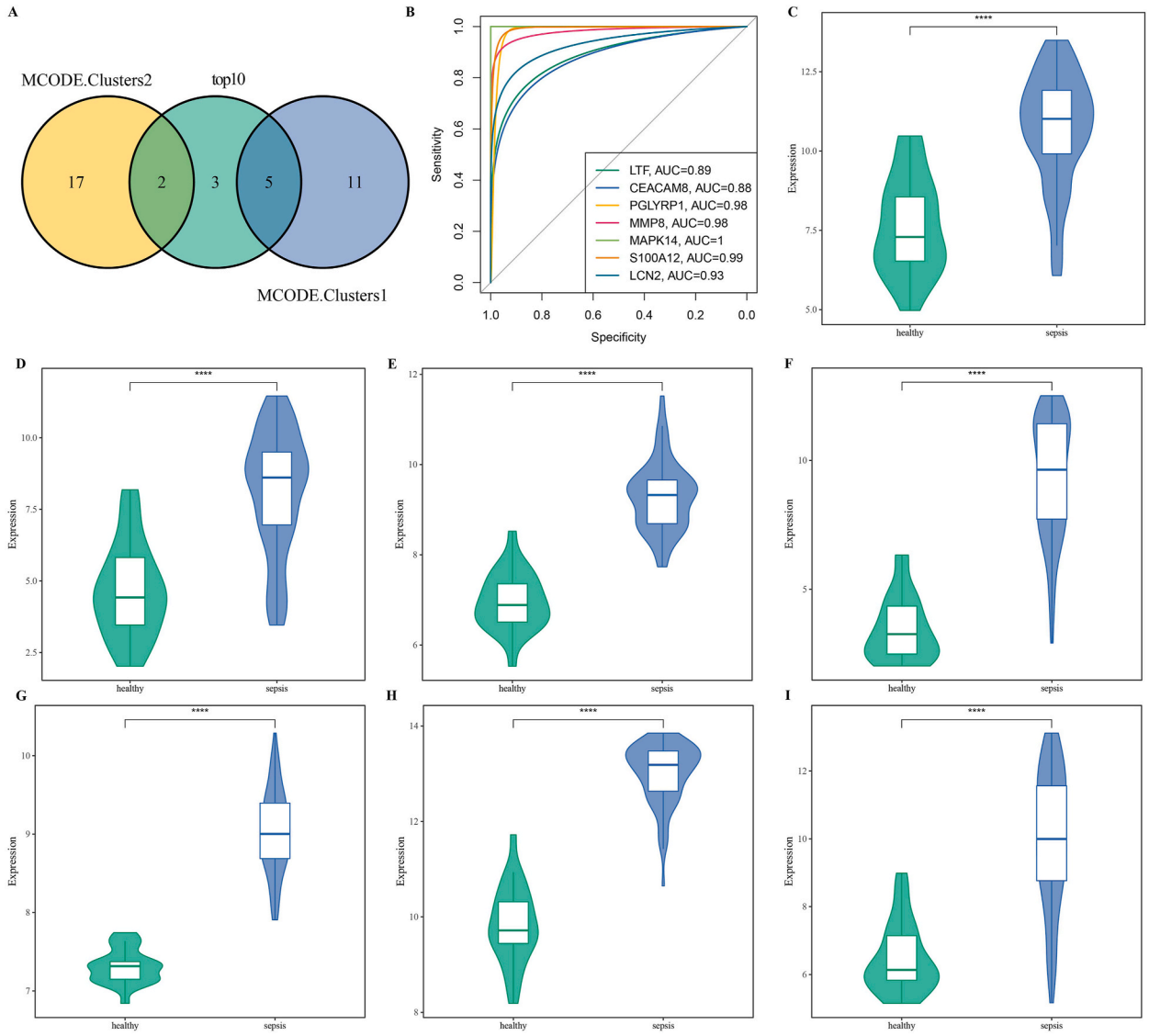

Fig. 5. Identification of NETosis associated genes.
A: NETosis associated genes; B: ROC analysis results of NETosis associated genes in the GSE57065 cohort; C–I: Expression differences of NETosis associated genes in different sample types in the GSE57065 cohort.

3.6. Relationship between NETosis-associated genes and immune infiltration and pathways

We analyzed the relationship between key genes of PPI network and different programmed death pathways, and found that these 7 genes were significantly positively correlated with netotic cell death, entotic cell death and ferroptosis and significantly negatively

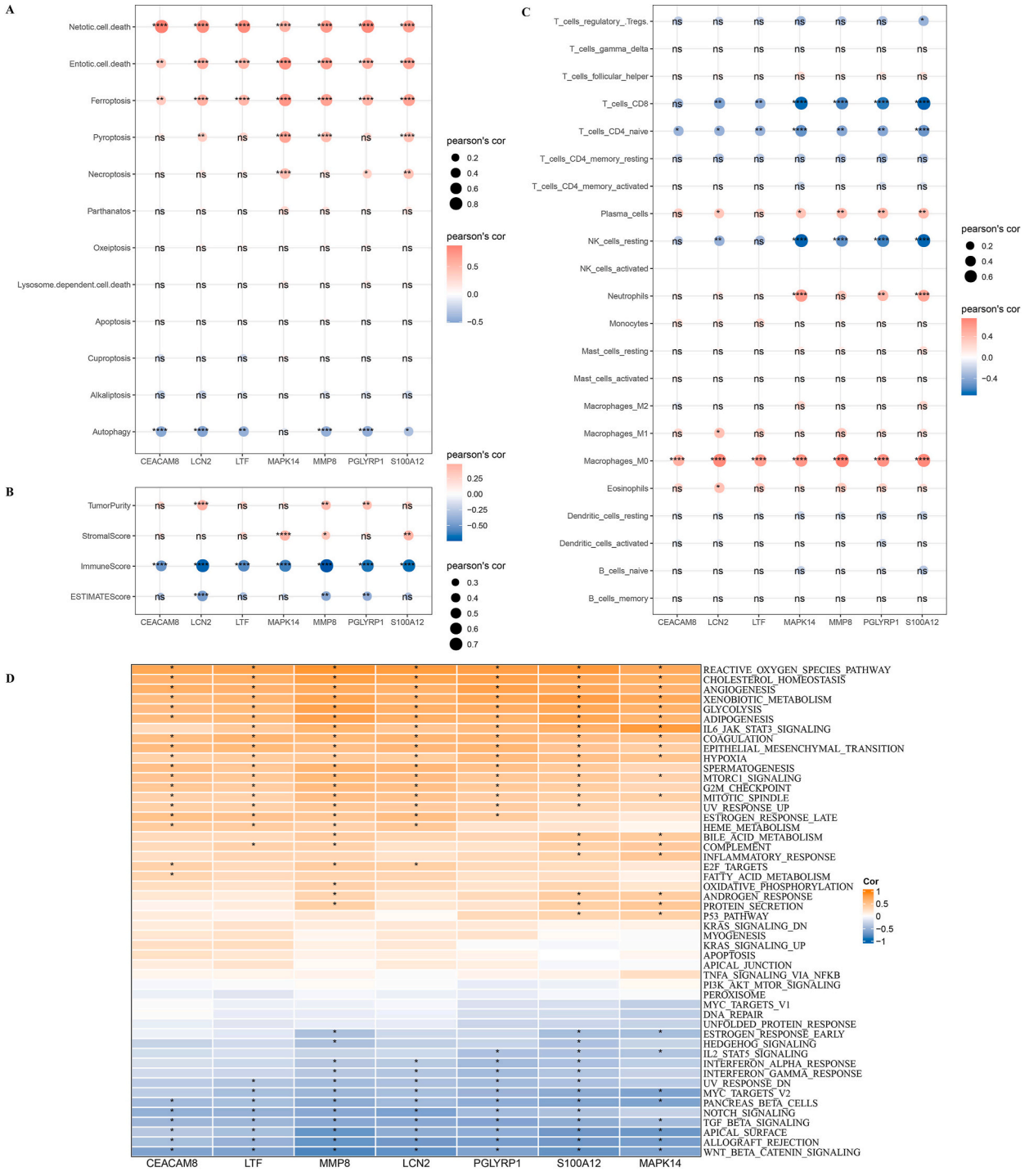

Fig. 6. Relationship between NETosis associated genes and immune infiltration and pathway.
A: Relationship between NETosis associated genes and different programmed death pathways in the GSE57065 cohort; B: The relationship between NETosis associated genes and immune infiltration in the GSE57065 cohort; C: The relationship between NETosis associated genes and different immune cells in the GSE57065 cohort; D: The relationship between NETosis associated genes and different pathways in the GSE57065 cohort.

correlated with autophagy (Fig. 6A). ImmuneScore was a biomarker assessed based on transcriptomic data to reflect the status of immune cell infiltration in tissues. Here, these 7 genes were significantly negatively correlated with ImmuneScore (Fig. 6B). This suggested that when the expression of these genes was increased, the ImmuneScore decreased, which indicated that there may be fewer immune cells infiltrating into the pathologic tissue. Furthermore, a significant negative correlation between these 7 genes and neutrophils and M0 macrophages was observed (Fig. 6C). These 7 genes were significantly positively correlated with cell cycle-related pathways such as G2M_CHECKPOINT, MITOTIC_SPINDLE, E2F_TARGETS, P53_PATHWAY and significantly posotively correlated with hypoxia, glycolysis, EMT, etc. (Fig. 6D).

3.7. Establishment and validation of a clinical prognostic model using NETosis-associated genes

Stepwise regression analysis was performed for the 7 NETosis-associated genes in the GSE65682 cohort. Finally, we identified 5 key

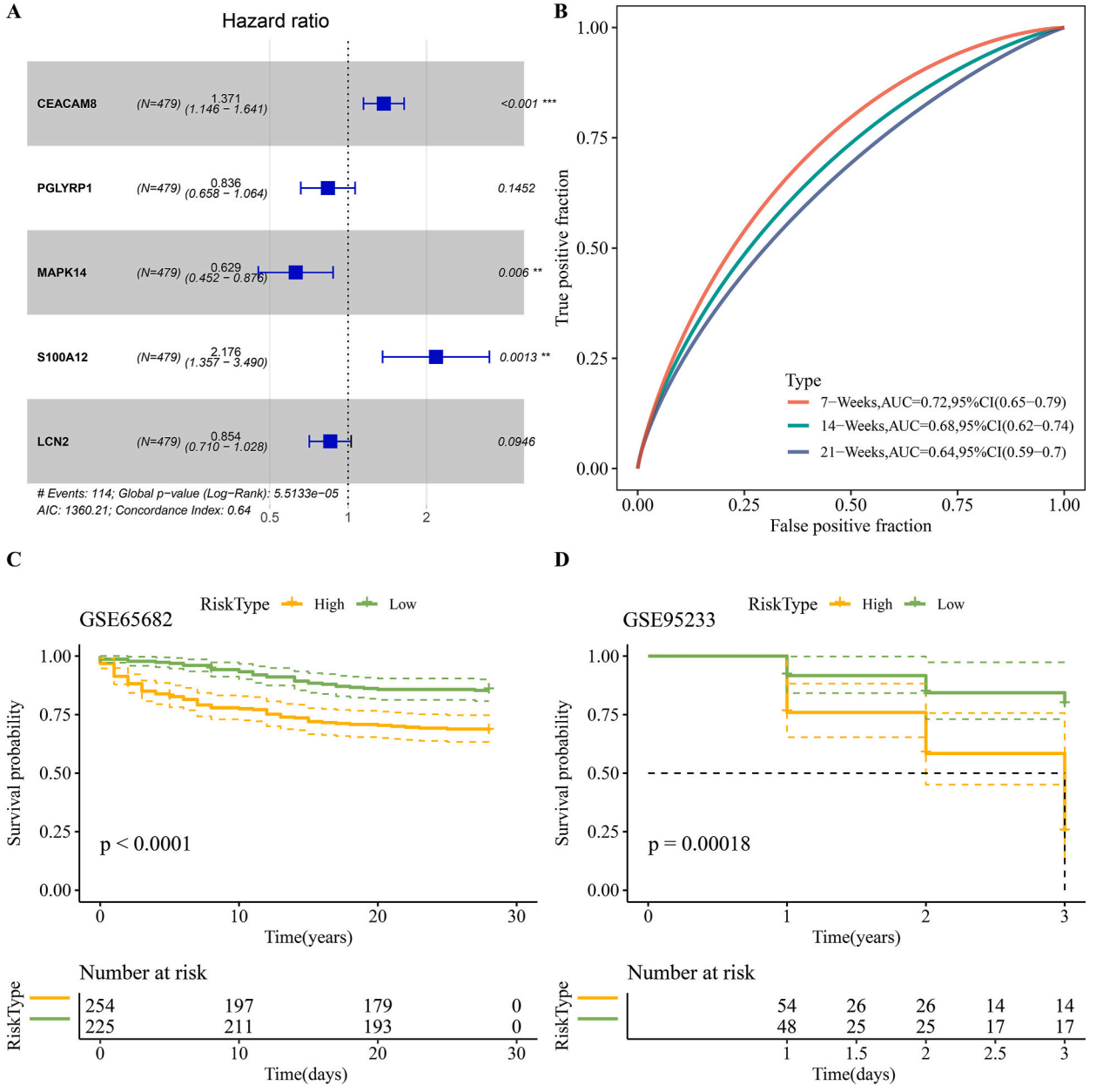

Fig. 7. Establishment and verification of clinical prognostic model based on NETosis associated genes.
A: Key gene of prognostic model; B: ROC curve and AUC of riskscore classification in GSE65682 data set; C: KM survival curve distribution in GSE65682 data set; D: riskscore distribution of KM curve in GSE95233 data set.

NETosis-associated genes (Fig. 7A). The final model formula was as follows:

Riskscore = 0.3157438 *CEACAM8-0.1785755 *PGLYRP1-0.4634681 *MAPK14 + 0.7774074*S100A12–0.1577366*LCN2

Then, according to the formula defined by our risk model, the riskscore of each sample in the GSE65682 cohort was calculated and the z-score was standardized. The classification efficiency of prognostic prediction was analyzed at 7 days, 14 days, and 21 days, respectively, and we observed that the AUC values of the three ROC curves were all high (Fig. 7B). Next, we compared the OS of patients with different riskscore. The results showed that the survival rate of patients with high riskscore was lower than that of patients with low riskscore. In addition, we found significant differences in OS ($p < 0.0001$) were found between the high group (254 samples) and low group (225 samples) (Fig. 7C).

For the robustness of the model prediction, we tested it in the GSE95233 cohort, and observed similar results in the validation cohort as in the GSE65682 cohort (Fig. 7D).

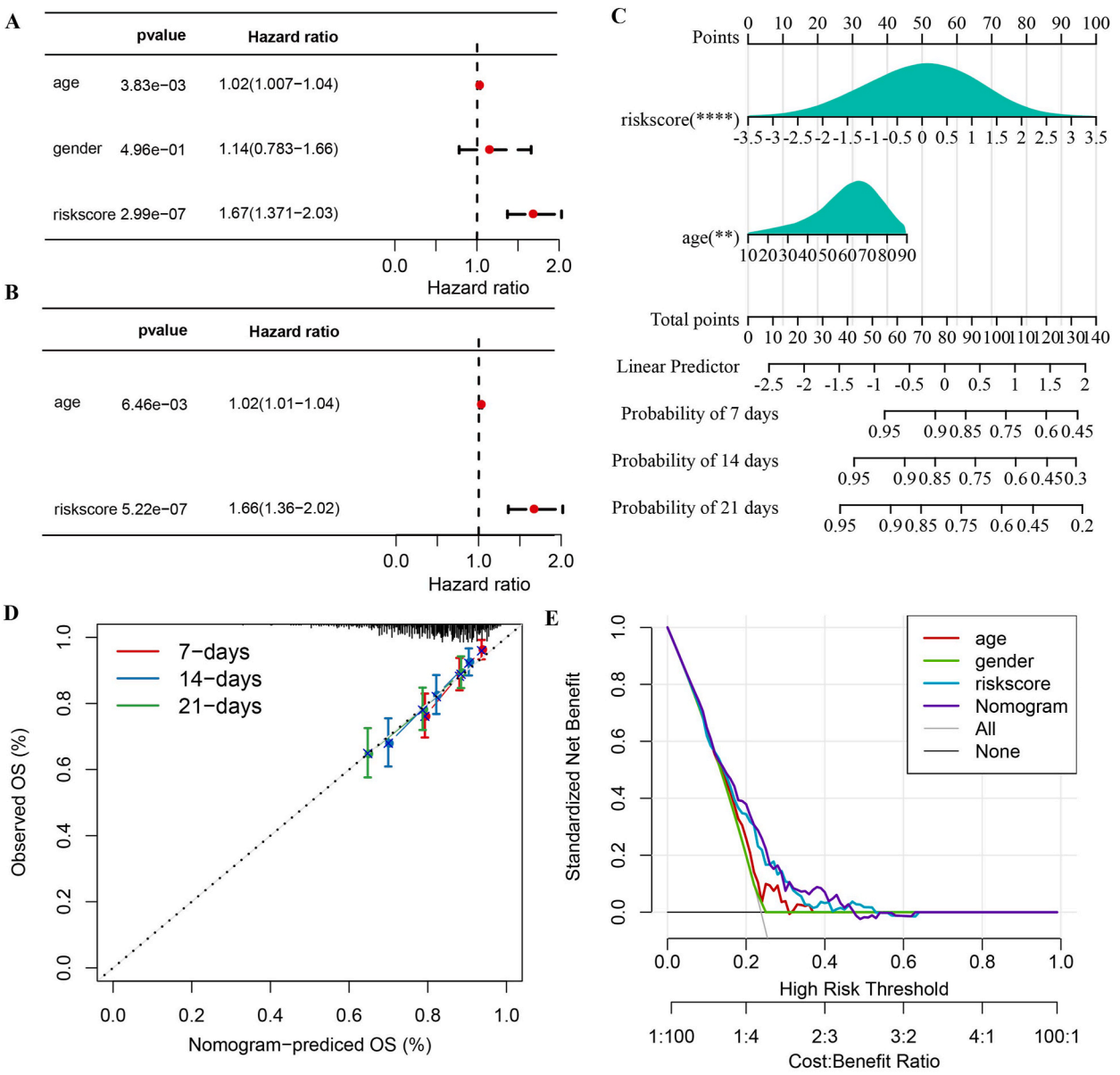

Fig. 8. Performance evaluation of the riskscore model.
A–B: Univariate and multivariate cox analysis results of riskscore and clinicopathological information in the GSE65682 cohort; C: Construction of nomogram; D: Calibration curves of the nomogram for 7 days, 14 days and 21 days; E: DCA curve of the nomogram.

3.8. Performance evaluation for the riskscore model

We performed univariate and multivariate Cox regression analyses for GSE65682. The analysis showed that the riskscore was significantly correlated with OS. Multivariate Cox analysis demonstrated that the riskscore could be used as an independent prognostic factor (Fig. 8A and B).

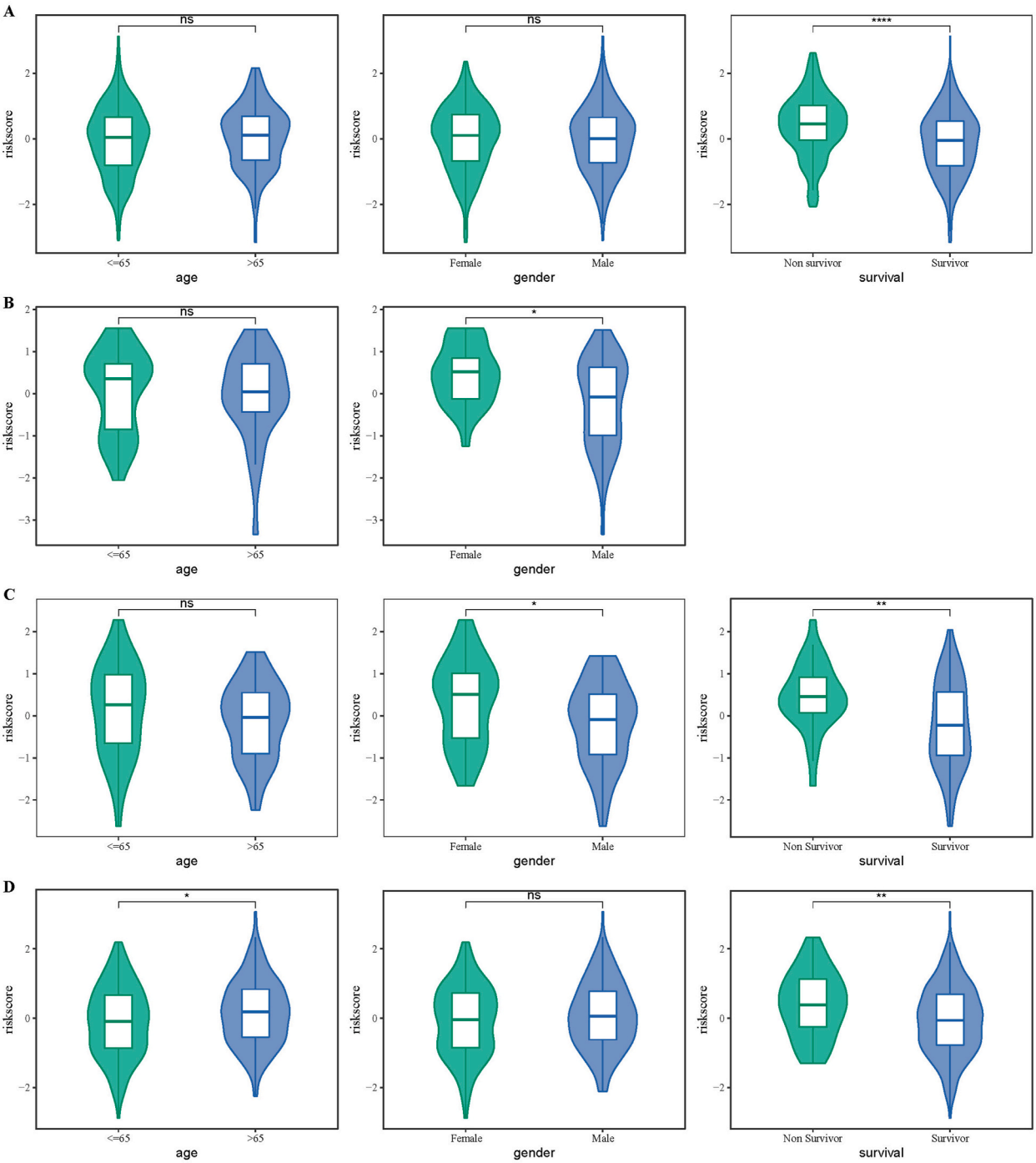

Fig. 9. Relationship between riskscore model and clinicopathological features.
A: The relationship between riskscore and clinicopathological features in the GSE65682 cohort; B: The relationship between riskscore and clinicopathological features in the GSE57065 cohort; C: The relationship between riskscore and clinicopathological features in the GSE95233 cohort; D: The relationship between riskscore and clinicopathological features in the GSE185263 cohort.

The riskscore was further combined with other clinicopathological characteristics to establish a nomogram. The model results indicated that the riskscore had the greatest impact on the prediction of survival rate (Fig. 8C). We further used Calibration curve to evaluate the prediction accuracy of the model. It can be observed that the prediction calibration curve of the three calibration points at 7 days, 14 days and 21 days was close to the standard curve, which indicated that the nomogram had a great prediction performance (Fig. 8D). In addition, Decision curve was used to evaluate the reliability of the model, and we observed that the riskscore and nomogram benefits were significantly higher than those of the extreme curve. Both the nomogram and riskscore showed the strongest survival prediction (Fig. 8E).

3.9. Relationship between the riskscore model and clinicopathologic features and immune infiltration in patients with sepsis

The relationship between the riskscore and clinicopathological features was explored. In GSE65682 dataset, patients with survivor state had a lower riskscore (Fig. 9A). In GSE57065 dataset, male patients presented a lower riskscore (Fig. 9B). While in GSE95233 dataset, male patients or patients with survivor state all had a decreased riskscore (Fig. 9C). Moreover, in GSE185263 dataset, younger patients and survivor patients had relatively lower riskscore (Fig. 9D).

The relationship between the riskscore and immune infiltration and pathways was evaluated based on the Pearson method. We calculated the correlation between the riskscore and various types of programmed death pathways, and found that riskscore was significantly positively correlated with netotic cell death ($p < 0.05$, Fig. 10A). Meanwhile, the riskscore was significantly positively correlated with M0 macrophages and Treg (Fig. 10B). In addition, it was found that the riskscore was significantly positively correlated with cell cycle-related pathways and negatively correlated with inflammatory pathways such as INTERFERON GAMMA RESPONSE and INTERFERON ALPHA RESPONSE (Fig. 10C).

4. Discussion

As a complex disease with abnormal response to infection, sepsis is closely related to the immunity of neutrophils [30]. Neutrophils have different types of death in sepsis, including apoptosis, NETosis, autophagy, and is related to their physiological role in sepsis [31,32]. Qianmin Ou et al. found that mesenchymal stem cells could generate apoptotic vesicles and transform the NETosis process in neutrophils into apoptosis, thereby improving the survival rate of sepsis [33]. Mohmad Alsabani et al. found that NETosis can be regulated by the gene signal CXCR1/2, reduce the secretion of NET, improve tissue damage, and attenuate the negative effects of sepsis [34].

This study identified five important NETosis-associated genes (CEACAM8, PGLYRP1, MAPK14, S100A12, and LCN2) that played important biological roles in sepsis. The carcinoembryonic antigen-related cell adhesion molecule 8 (CEACAM8) is an important cell adhesion molecule in neutrophils. When neutrophils receive external stimulation, CEACAM8 will be released and expressed [35]. Zhihao Xu et al. showed that the mRNA expression level of CEACAM8 is significantly elevated in mice and human models with sepsis, suggesting that the gene could serve as a potential biomarker for sepsis [36]. Peptidoglycan recognition protein 1 (PGLYRP1) is a defense gene implicated in the body's inflammatory response and is usually up-regulated in patients with infection and injury [37,38]. Fangchen Gong et al. found that the tissue expression level of PGLYRP1 is somewhat correlated with sepsis and may also serve as a new diagnostic gene for sepsis [39].

The mitogen-activated protein kinase 14 (MAPK14) plays a crucial role in inflammation, various cancers and sepsis [40,41]. MAPK14 is involved in endocytosis of membrane receptors in sepsis to facilitate EGFR transport and improve phenotypic transformation of macrophages [42]. S100A12 is a calc-binding protein secreted by neutrophils that can activate the body's immune response by participating in intracellular inflammation and immune-related signaling [43]. S100A12 has a high expression level under inflammation, and as a pro-inflammatory factor, it can bind to corresponding receptors to help induce monocyte activation [44]. Lipocalin-2 (Lcn2) is an innate immune protein that promotes macrophage inactivation and induces immune cell apoptosis to reduce immune overshooting in sepsis and help eliminate the negative effects of immune defense [45]. In sepsis patients, the transcription factor FRA-1 binds to the Lcn2 promoter, inhibits the secretion of anti-inflammatory factors, increases the infiltration of neutrophils, thereby suppressing the inflammatory response [46].

The role of neutrophils in patients with early and late sepsis is quite different. Early activated neutrophils release NETs that help capture pathogens in the microenvironment and induce pro-inflammatory transition of endothelial cells to fight against infection [47]. NET produced by neutrophils can also promote endoplasmic reticulum stress response, increase apoptosis of infected tissue cells, and cause tissue damage [48]. After receiving regulation such as inhibiting apoptosis and inhibiting T cell activation, neutrophils in advanced patients exhibit immunosuppressive states that could help patients avoid immune-induced tissue damage [49].

There were still some limitations in this study. The experimental data all came from GEO database and the sample size was relatively small. In the future, it is necessary to expand the sample size and combine multiple databases to carry out a more comprehensive study. This study also lacked clinical trials and related cell experiments to verify the findings, therefore we will combine more clinical data and perform cell experiments to provide pathological research on sepsis.

5. Conclusion

This study identified five NETosis-associated genes (CEACAM8, PGLYRP1, MAPK14, S100A12, and LCN2) through WGCNA and PPI network analysis. A clinical prognostic model based on the riskscore was established, which had a strong stability and prediction ability. This study not only preliminarily revealed the important role of NETosis in sepsis, but also provided new biomarkers and

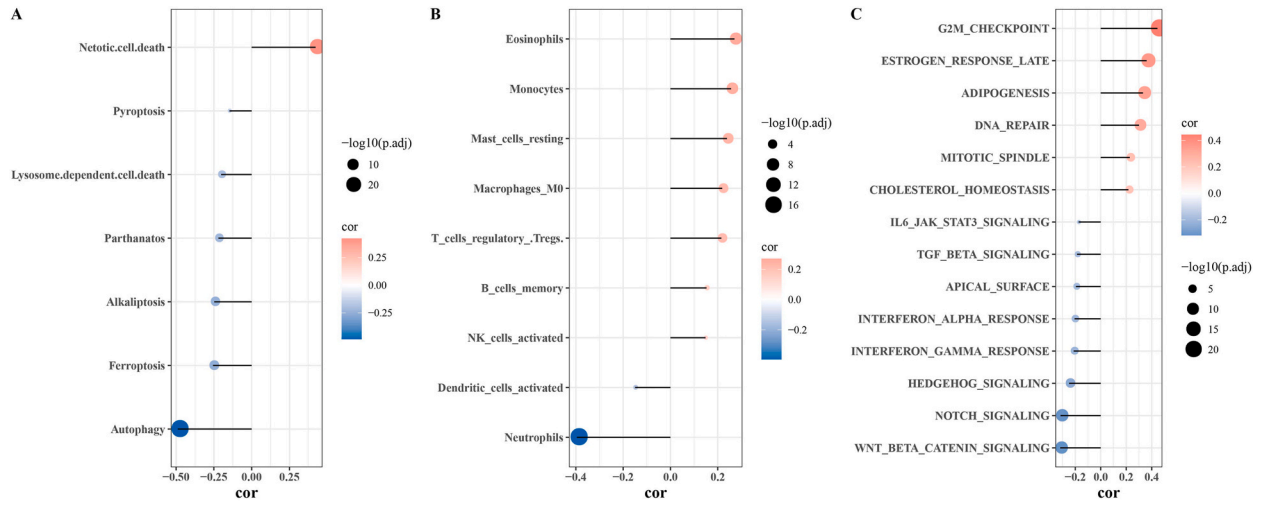

Fig. 10. Relationship between risk model and immune infiltration and pathway.
A: The relationship between riskscore and programmed death pathway in the GSE65682 cohort; B: The relationship between riskscore and immune cells in GSE65682 cohort; C: The relationship between riskscore and HALLMARK pathway in GSE65682 cohort.

potential therapeutic targets, which are important for improving the diagnosis and individualized treatment of sepsis.

Funding

This research did not receive any specific grant from funding agencies in the public, commercial, or not-for-profit sectors.

Data availability statement

The datasets generated and/or analyzed during the current study are available in the [GSE57065] repository, [https://www.ncbi.nlm.nih.gov/geo/query/acc.cgi?acc= GSE57065], [GSE95233] repository, [https://www.ncbi.nlm.nih.gov/geo/query/acc.cgi?acc= GSE95233], [GSE185263] repository [https://www.ncbi.nlm.nih.gov/geo/query/acc.cgi?acc= GSE185263], and [GSE65682] repository, [https://www.ncbi.nlm.nih.gov/geo/query/acc.cgi?acc= GSE65682]. The code used by the institute to the Github platform with the repository URL: https://github.com/LinghuiHuang/code.git.

Ethical statement

Informed consent was not required for this study because it is not involved any human experiments.

CRediT authorship contribution statement

Jiahao Wu: Writing – review & editing, Writing – original draft, Software, Resources, Project administration. **Xingxing Cao:** Writing – review & editing, Writing – original draft, Visualization, Supervision, Formal analysis, Data curation, Conceptualization. **Linghui Huang:** Validation, Software, Project administration, Investigation, Conceptualization. **Yifeng Quan:** Visualization, Software, Methodology, Investigation, Formal analysis.

Declaration of competing interest

The authors declare that they have no known competing financial interests or personal relationships that could have appeared to influence the work reported in this paper.

Acknowledgments

None.

Appendix A. Supplementary data

Supplementary data to this article can be found online at https://doi.org/10.1016/j.heliyon.2024.e36831.

Abbreviations

GEO	Gene Expression Omnibus
PPI	Protein-Protein Interaction
GSEA	gene set enrichment analysis
ssGSEA	single sample gene set enrichment analysis
WGCNA	weighted corrVelation network analysis
EMT	epithelial-mesenchymal transition
OS	overall survival
MsigDB	The Molecular Signatures Database
MAD	Median Absolute Deviation
TOM	topological overlap matrix
NET	neutrophils extracellular trap
GS	gene significance
MM	module membership
CEACAM8	The carcinoembryonic antigen-related cell adhesion molecule 8
PGLYRP1	Peptidoglycan recognition protein 1
MAPK14	The mitogen-activated protein kinase 14
Lcn2	Lipocalin-2

References

[1] K.E. Rudd, et al., Global, regional, and national sepsis incidence and mortality, 1990-2017: analysis for the Global Burden of Disease Study, Lancet 395 (10219) (2020) 200–211.
[2] V. Liu, et al., Hospital deaths in patients with sepsis from 2 independent cohorts, JAMA 312 (1) (2014) 90–92.
[3] M. Singer, et al., The third international consensus definitions for sepsis and septic shock (Sepsis-3), JAMA 315 (8) (2016) 801–810.
[4] D. Thorrington, et al., Elucidating the impact of the pneumococcal conjugate vaccine programme on pneumonia, sepsis and otitis media hospital admissions in England using a composite control, BMC Med. 16 (1) (2018) 13.
[5] R. Martischang, et al., Promoting and sustaining a historical and global effort to prevent sepsis: the 2018 World Health Organization SAVE LIVES: clean Your Hands campaign, Crit. Care 22 (1) (2018) 92.
[6] M. Luo, et al., LGALS3BP: a potential plasma biomarker associated with diagnosis and prognosis in patients with sepsis, Infect. Drug Resist. 14 (2021) 2863–2871.
[7] S.L. Weiss, et al., Surviving sepsis campaign international guidelines for the management of septic shock and sepsis-associated organ dysfunction in children, Intensive Care Med. 46 (Suppl 1) (2020) 10–67.
[8] A. Rhodes, et al., Surviving sepsis campaign: international guidelines for management of sepsis and septic shock: 2016, Intensive Care Med. 43 (3) (2017) 304–377.
[9] C.M. de Bont, W.C. Boelens, G.J.M. Pruijn, NETosis, complement, and coagulation: a triangular relationship, Cell. Mol. Immunol. 16 (1) (2019) 19–27.
[10] H.R. Thiam, et al., Cellular mechanisms of NETosis, Annu. Rev. Cell Dev. Biol. 36 (2020) 191–218.
[11] N.V. Vorobjeva, B.V. Chernyak, NETosis: molecular mechanisms, role in physiology and pathology, Biochemistry (Mosc.) 85 (10) (2020) 1178–1190.
[12] T. Chen, et al., Receptor-mediated NETosis on neutrophils, Front. Immunol. 12 (2021) 775267.
[13] M. Sabbatini, V. Magnelli, F. Renò, NETosis in wound healing: when enough is enough, Cells 10 (3) (2021).
[14] D. Toro-Domínguez, et al., ImaGEO: integrative gene expression meta-analysis from GEO database, Bioinformatics 35 (5) (2019) 880–882.
[15] M.L. Wilhelm, et al., Tumor-dose-rate variations during robotic radiosurgery of oligo and multiple brain metastases, Strahlenther. Onkol. 197 (7) (2021) 581–591.
[16] M. Mohammadi-Dehcheshmeh, et al., Unified transcriptomic signature of arbuscular mycorrhiza colonization in roots of medicago truncatula by integration of machine learning, promoter analysis, and direct merging meta-analysis, Front. Plant Sci. 9 (2018) 1550.
[17] Y. Zou, et al., Leveraging diverse cell-death patterns to predict the prognosis and drug sensitivity of triple-negative breast cancer patients after surgery, Int. J. Surg. 107 (2022) 106936.
[18] Q. Wu, et al., Astrocytic YAP protects the optic nerve and retina in an experimental autoimmune encephalomyelitis model through TGF-β signaling, Theranostics 11 (17) (2021) 8480–8499.
[19] AS Castanza, JM Recla, D Eby, H Thorvaldsdóttir, CJ Bult, JP Mesirov, Extending support for mouse data in the Molecular Signatures Database (MSigDB), Nat Methods 20 (11) (2023 Nov) 1619–1620, https://doi.org/10.1038/s41592-023-02014-7. PMID: 37704782.
[20] T. Wu, et al., clusterProfiler 4.0: a universal enrichment tool for interpreting omics data, Innovation 2 (3) (2021) 100141.
[21] X. Liu, et al., Identification of LTF as a prognostic biomarker for osteosarcoma, J Oncol 2022 (2022) 4656661.
[22] J. Zhang, et al., High expression level of the FTH1 gene is associated with poor prognosis in children with non-M3 acute myeloid leukemia, Front. Oncol. 12 (2022) 1068094.
[23] S. Feng, et al., Integrative analysis from multicenter studies identifies a WGCNA-derived cancer-associated fibroblast signature for ovarian cancer, Front. Immunol. 13 (2022) 951582.
[24] M. Fang, et al., WGCNA and LASSO algorithm constructed an immune infiltration-related 5-gene signature and nomogram to improve prognosis prediction of hepatocellular carcinoma, Biocell 46 (2) (2022) 401–415.
[25] N. Murtaza, et al., Neuron-specific protein network mapping of autism risk genes identifies shared biological mechanisms and disease-relevant pathologies, Cell Rep. 41 (8) (2022) 111678.
[26] X.P. Zhang, et al., A novel online calculator to predict early recurrence and long-term survival of patients with resectable pancreatic ductal adenocarcinoma after pancreaticoduodenectomy: a multicenter study, Int. J. Surg. 106 (2022) 106891.
[27] K. Yoshihara, et al., Inferring tumour purity and stromal and immune cell admixture from expression data, Nat. Commun. 4 (2013) 2612.
[28] B. Chen, et al., Profiling tumor infiltrating immune cells with CIBERSORT, Methods Mol. Biol. 1711 (2018) 243–259.
[29] W. Shen, et al., Sangerbox: a comprehensive, interaction-friendly clinical bioinformatics analysis platform, Imeta 1 (3) (2022) e36.
[30] H.J. Hamam, N. Palaniyar, Post-translational modifications in NETosis and NETs-mediated diseases, Biomolecules 9 (8) (2019).
[31] C.L. Zhu, et al., Dysregulation of neutrophil death in sepsis, Front. Immunol. 13 (2022) 963955.

[32] H.P. Foote, et al., Using pharmacokinetic modeling and electronic health record data to predict clinical and safety outcomes after methylprednisolone exposure during cardiopulmonary bypass in neonates, Congenit. Heart Dis. 18 (3) (2023) 295–313.
[33] Q. Ou, et al., Electrostatic charge-mediated apoptotic vesicle biodistribution attenuates sepsis by switching neutrophil NETosis to apoptosis, Small 18 (20) (2022) 2200306.
[34] M. Alsabani, et al., Reduction of NETosis by targeting CXCR1/2 reduces thrombosis, lung injury, and mortality in experimental human and murine sepsis, Br. J. Anaesth. 128 (2) (2022) 283–293.
[35] L. Xiao, W. Xiao, S. Lin, Potential biomarkers for active renal involvement in systemic lupus erythematosus patients, Front. Med. 9 (2022) 995103.
[36] Z. Xu, et al., Identification and verification of potential core genes in pediatric septic shock, Comb. Chem. High Throughput Screen. 25 (13) (2022) 2228–2239.
[37] A Silbereisen, R Lira-Junior, S Åkerman, B Klinge, EA Boström, N Bostanci, Association of salivary TREM-1 and PGLYRP1 inflammatory markers with non-communicable diseases, J Clin Periodontol 50 (11) (2023 Nov) 1467–1475, https://doi.org/10.1111/jcpe.13858. Epub 2023 Jul 31. PMID: 37524498.
[38] Y. Jia, et al., PGLYRP1-mIgG2a-Fc inhibits macrophage activation via AKT/NF-κB signaling and protects against fatal lung injury during bacterial infection, iScience 26 (5) (2023) 106653.
[39] F. Gong, et al., OLFM4 regulates lung epithelial cell function in sepsis-associated ARDS/ALI via LDHA-mediated NF-κB signaling, J. Inflamm. Res. 14 (2021) 7035–7051.
[40] M.M. Madkour, H.S. Anbar, M.I. El-Gamal, Current status and future prospects of p38α/MAPK14 kinase and its inhibitors, Eur. J. Med. Chem. 213 (2021) 113216.
[41] X. Liu, et al., LINC00839 promotes colorectal cancer progression by recruiting RUVBL1/Tip60 complexes to activate NRF1, EMBO Rep. 23 (9) (2022) e54128.
[42] X. Zhang, et al., EGFR tyrosine kinase activity and Rab GTPases coordinate EGFR trafficking to regulate macrophage activation in sepsis, Cell Death Dis. 13 (11) (2022) 934.
[43] A. Nazari, et al., S100A12 in renal and cardiovascular diseases, Life Sci. 191 (2017) 253–258.
[44] D. Foell, et al., Proinflammatory S100A12 can activate human monocytes via Toll-like receptor 4, Am. J. Respir. Crit. Care Med. 187 (12) (2013) 1324–1334.
[45] F. Lu, et al., Functions and regulation of lipocalin-2 in gut-origin sepsis: a narrative review, Crit. Care 23 (1) (2019) 269.
[46] S. Cao, et al., The transcription factor FRA-1/AP-1 controls lipocalin-2 expression and inflammation in sepsis model, Front. Immunol. 12 (2021) 701675.
[47] H. Zhang, et al., Neutrophil, neutrophil extracellular traps and endothelial cell dysfunction in sepsis, Clin. Transl. Med. 13 (1) (2023) e1170.
[48] S. Sun, et al., Neutrophil extracellular traps impair intestinal barrier functions in sepsis by regulating TLR9-mediated endoplasmic reticulum stress pathway, Cell Death Dis. 12 (6) (2021) 606.
[49] X. Qi, et al., Identification and characterization of neutrophil heterogeneity in sepsis, Crit. Care 25 (1) (2021) 50.